# C, CO and $CO_2$ hydrogenation on cobalt foil model catalysts: evidence for the need of CoO reduction

J. Lahtinen [1], T. Anraku [2] and G.A. Somorjai

*Materials Science Division, Lawrence Berkeley Laboratory and Department of Chemistry, University of California, Berkeley, CA 94720, USA*

Received 12 October 1993; accepted 16 January 1994

The hydrogenation of C, CO, and $CO_2$ has been studied on polycrystalline cobalt foils using a combination of UHV studies and atmospheric pressure reactions in temperature range from 475 to 575 K at 101 kPa total pressure. The reactions produce mainly methane but with selectivities of 98, 80, and 99 wt% at 525 K for C, CO, and $CO_2$, respectively. In the C and $CO_2$ hydrogenation the rest is ethane, whereas in CO hydrogenation hydrocarbons up to $C_4$ were detected. The activation energies of methane formation are 57, 86, and 158 kJ/mol from C, CO, and $CO_2$, respectively. The partial pressure dependencies of the CO and $CO_2$ hydrogenation indicate roughly first order dependence on hydrogen pressure (1.5 and 0.9), negative first order on CO (−0.75) and zero order on $CO_2$ (−0.05). Post reaction spectroscopy revealed carbon deposition from CO and oxygen deposition from $CO_2$ on the surface above 540 K. The reduction of cobalt oxide formed after dissociation of C–O bonds on the surface is proposed to be the rate limiting step in CO and $CO_2$ hydrogenation.

**Keywords:** C, CO, and $CO_2$ hydrogenation; cobalt catalysts

## 1. Introduction

Cobalt has been used as an important catalyst from the early days of carbon monoxide hydrogenation studies [1,2]. However, its use in model catalytic studies to explore the elementary reaction steps from the surface science viewpoint have not been explored when compared to studies of this type on iron [3,4], nickel [5,6], and rhodium [7,8]. In these investigations the dissociation of CO to carbon and oxygen was found to be a dominant reaction step followed by the hydrogenation of carbon to methane and other reaction products [4,6,8,9].

In order to explore the differences between cobalt chemistry and the surface

[1] Laboratory of Physics, Helsinki University of Technology, 02150 Espoo, Finland.
[2] Corrosion Research Laboratory, Sumitomo Metal Industries, Ltd., 8, 1, Fusoh-Cho, Amagasaki, 660 Japan.

chemistry of the other transition metals, we have studied the hydrogenation of carbon, CO, and $CO_2$ over cobalt foils in the temperature range from 475 to 575 K at 101 kPa (760 Torr). The reactions yield predominantly methane and the rates show roughly first order dependence on hydrogen pressure (1.5 and 0.9), negative order dependence on CO (−0.75), and zero order dependence on $CO_2$ concentration (−0.05). The activation energies for the three hydrogenation processes increase steeply with oxygen content of the carbon species; it is 57 kJ/mol for C, 86 kJ/mol for CO, and 158 kJ/mol for $CO_2$ hydrogenation.

The hydrogenation of CO on cobalt proceeds via dissociation of CO and subsequent hydrogenation of carbon to methane [10–13]. Several reaction mechanisms for the $CO_2$ hydrogenation have been proposed including direct hydrogenation of $CO_2$ [14], dissociation to CO and O [14], or to C and 2O [5,15] prior to the methane formation. On Ni surfaces the reaction is reported to proceed via dissociation to C and 2O and subsequent hydrogenation of surface carbon to methane [5,15]. Our results support this reaction path also on cobalt foils.

The increase in the activation energy with increasing oxygen content can be explained if we consider the facile formation of cobalt oxide during CO and $CO_2$ dissociation. Because of the strong Co–O bond the reactions $CO + Co \rightarrow C + CoO$ and $CO_2 + 2Co \rightarrow C + 2CoO$ are exothermic ($\Delta H = -129$ and $-85.5$ kJ/mol, respectively). The hydrogenation of carbon can only occur, it appears, if Co–O is reduced also during the process. Thus the large activation energy for $CO_2$ hydrogenation to methane includes the activation energies for the reduction of two Co–O species. The activation energy for CO hydrogenation to methane includes the reduction of one Co–O species. These proposals are in agreement with the recent findings of Iglesia et al. where they find that addition of Ru on supported cobalt catalysts enhances the activity of the catalysts mainly by affecting the reducibility of cobalt [16].

## 2. Experimental

The research was carried out in a combined ultrahigh vacuum (UHV) atmospheric pressure chamber pumped with a diffusion pump and equipped with a double-pass cylindrical mirror analyzer, a 3 keV sputter ion gun and a quadrupole mass spectrometer. For catalytic reaction rate studies the sample was enclosed in a special isolation cell that constitutes part of a microbatch reactor operating at atmospheric pressures. Products generated during the reaction experiments were separated with a gas chromatograph. The system is described in more details elsewhere [12,17].

The reactants were introduced via a gas handling manifold where the pressure was measured with a differential pressure gauge. The purities of the gases used in the experiments were 99.5% (CO), 99.95% ($CO_2$), and 99.99% ($H_2$ and Ar) and the

gases were cleaned prior to use by passing them through liquid nitrogen cooled molecular sieve traps as described earlier [12].

The cobalt samples were 125 μm thick high purity foil with surface areas $< 1$ cm$^2$ spotwelded on 0.9 mm Au wires connected to copper supports. The sample temperature was measured via a chromel–alumel thermocouple spotwelded on the backside of the sample and maintained using a proportional temperature controller within ±3 K.

Prior to experiments both faces of the samples were cleaned by $Ar^+$ sputtering followed by $H_2$ exposure at 101 kPa for several hours to react with the carbon segregating to the surface. When the samples were annealed after sputtering small amounts of carbon segregated to the surface. After the reaction rate measurements the surface was cleaned by sputtering followed by annealing at 770 K.

## 3. Results

### 3.1. HYDROGENATION OF CARBON DIFFUSED FROM COBALT BULK ONTO THE SURFACE

Hydrogenation of carbon diffused from cobalt bulk onto the surface was investigated in the temperature range from 450 to 560 K on cobalt foils. The rate of methane formation at 525 K was 0.022 methane molecules produced per cobalt site per second. The geometrical surface area of the sample with $10^{15}$ atoms/cm$^2$ was used to estimate the initial turnover number from the accumulated methane versus time data.

The turnover rate is plotted in fig. 1 as a function of the inverse temperature.

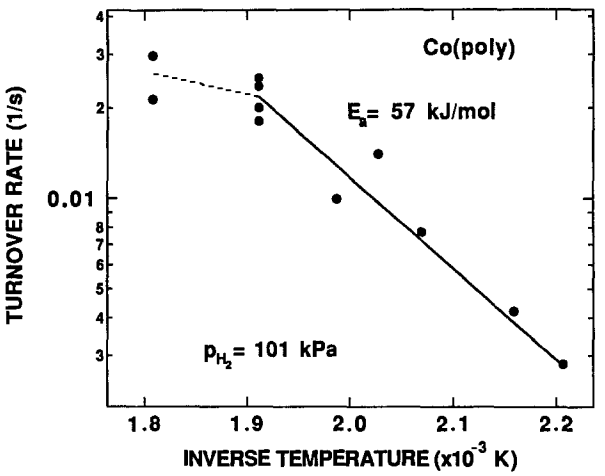


Fig. 1. The initial rate of methane formation from carbon as a function of inverse temperature on cobalt foil. The $H_2$ pressure was 101 kPa. The solid line is drawn for an activation energy of 57 kJ/mol.

The data points in the figure fall relatively well on the solid line representing an activation energy of 57 ± 3 kJ/mol except at temperatures exceeding 530 K where the activity starts to level off.

The product distribution from the carbon hydrogenation showed 98 wt% methane and 2 wt% ethane above 500 K, and only methane at temperatures lower than 500 K. The product distribution at 525 K is shown in fig. 2.

The sample surface was characterized with AES immediately after termination of the reaction and opening of the cell. The Auger spectra revealed few at% carbon on the surface but the small peak heights prevented us to distinguish the chemical state of the surface carbon after the reaction. In general the amount of carbon decreased during the hydrogenation and these reactions were also used to clean the sample bulk.

### 3.2. HYDROGENATION OF CARBON MONOXIDE OVER COBALT FOILS

The catalytic hydrogenation of carbon monoxide was investigated in the temperature range from 475 to 570 K. The initial rates of methane formation at 525 K, when the $H_2/CO$ ratio was 3 and the total pressure 101 kPa (760 Torr), was 0.33 methane molecules produced per cobalt site per second.

The activation energy for methane formation was 86 ± 7 kJ/mol when determined from the initial rate of methane formation versus inverse temperature. The product distribution shown in fig. 2 indicated 80 wt% methane, 10.5 wt% $C_2$, 6 wt% $C_3$, and 2.3 wt% of $C_4$ species.

The dependence of the rate of methane formation on the partial pressures of

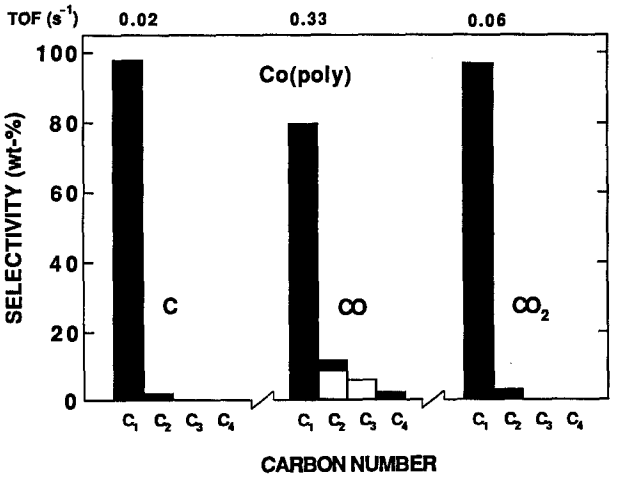


Fig. 2. The product distributions from hydrogenation of C, CO and $CO_2$ at 525 K. The hydrogen pressure was 76 kPa for CO and $CO_2$ hydrogenation and 101 kPa for C hydrogenation, and the CO or $CO_2$ pressure 25 kPa. The black columns represent alkanes whereas the alkene fractions are denoted by white area.

the reactants at 525 K were determined by varying the partial pressure of both reactant gases independently while maintaining the total pressure at 101 kPa using argon as a fill-up gas. The data is shown in fig. 3. For CO pressure dependence measurements the $H_2$ pressure was held at 56 kPa (420 Torr) and for the $H_2$ pressure dependence measurements the CO pressure was held at 25 kPa (190 Torr). The measured data was fitted to equation

$$r_{CH_4} = k p_{H_2}^{\alpha} p_{CO}^{\beta} \quad (1)$$

to determine the coefficients $\alpha$ and $\beta$ for $H_2$ and CO pressure dependencies. Values of $\alpha = 1.5$ for $H_2$ pressures between 12 and 76 kPa and $\beta = -0.75$ for CO pressure from 3.5 to 45 kPa were obtained.

The surface compositions of the samples were characterized by AES immediately after opening the reaction cell without any further heating of the sample. The spectra showed variable amounts of oxygen and carbon deposited on the surface. In fig. 4 the C/Co and O/Co AES peak height ratios are plotted with solid circles as a function of reaction temperature. The data indicate that the amount of oxygen slightly decreases as the temperature increases whereas the deposition of carbon starts to increase above 540 K with simultaneous onset of graphite formation. A more detailed analysis of the CO hydrogenation data has been given elsewhere [12,18,19].

### 3.3. HYDROGENATION OF CARBON DIOXIDE OVER COBALT FOILS

The catalytic hydrogenation of carbon dioxide was investigated in the temperature range from 475 to 575 K. The initial rates of methane formation at 525 and

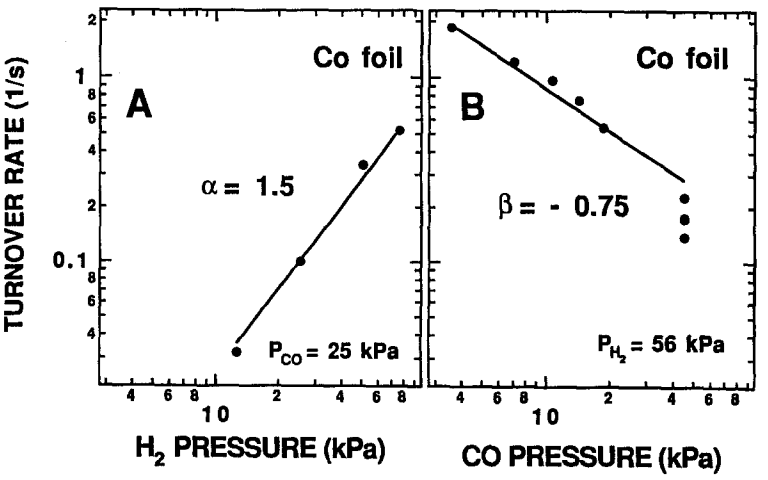


Fig. 3. Hydrogen (A) and carbon monoxide (B) partial pressure dependence on the rate of methane formation on cobalt foil. The reaction temperature was 525 K and the total pressure 101 kPa. The solid lines were drawn using eq. (1) with exponent values $\alpha = 1.5$ and $\beta = -0.75$.

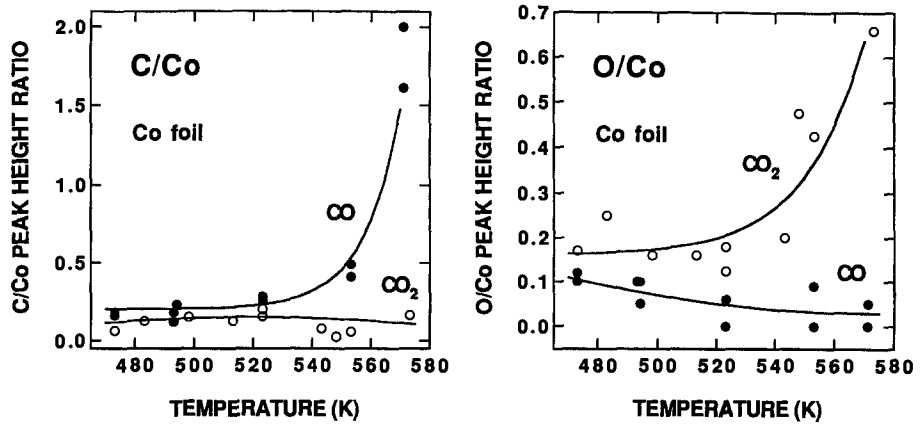


Fig. 4. Carbon to cobalt and oxygen to cobalt Auger peak height ratios after the reaction experiments as a function of reaction temperature. The black circles are measured after CO hydrogenation and the open circles after $CO_2$ hydrogenation. The gas composition featured $H_2/CO$ ratio of 1.24 and $H_2/CO_2$ ratio of 3 at 101 kPa. The solid lines are drawn to guide the eye.

575 K when the $H_2/CO_2$ ratio was 3 and the total pressure 101 kPa (760 Torr) were 0.064 and 1.55 methane molecules produced per cobalt site per second, respectively.

The Arrhenius plots for the $CO_2$ hydrogenation are plotted in fig. 5. The data

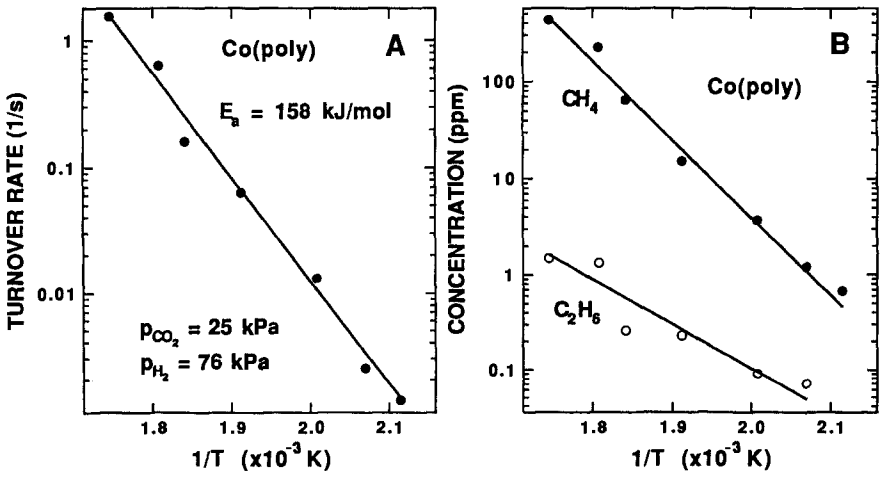


Fig. 5. The initial rate of methane formation (A) and the accumulated amount of methane and ethane after 1 h reaction (B) as a function of inverse temperature on cobalt foil during $CO_2$ hydrogenation. The $H_2/CO_2$ ratio was 3 and the total pressure 101 kPa. The solid line in (A) is drawn for an activation energy of 158 kJ/mol, whereas the solid lines in (B) are obtained with values of 155 kJ/mol for methane and 90 kJ/mol for ethane.

have been obtained by varying the sample temperature while holding the total pressure and reactant gas composition constant ($P_{H_2} = 76$ kPa, $P_{CO_2} = 25$ kPa). The solid line in the initial methane formation rate data in fig. 5A represents an activation energy of $158 \pm 6$ kJ/mol. In fig. 5B is plotted the concentration of methane and ethane after 1 h reaction time. The activation energies for methane and ethane formation when determined from the data taken after 1 h reaction time are $155 \pm 5$ and $90 \pm 5$ kJ/mol, respectively. No other hydrocarbons could be detected during the reaction.

The product distributions after 1 h reaction time at various temperatures are given in table 1. It can be seen that the selectivity towards methane increases from 95 to 99% when the reaction temperature increases from 500 to 560 K. The rest of the products are ethane. In table 1 is also shown the product distributions at 525 K when the $H_2/CO_2$ ratio was changed from 2 to 4. In this case the selectivity to methane increases from 96 to 98% and the rest was ethane. Fig. 2 gives the product distribution at 525 K with $H_2/CO_2$ ratio of 3.

The dependence of the rate of methane formation on the partial pressures of the reactants was determined by varying the partial pressure of both reactant gases independently while maintaining the total pressure at 101 kPa using argon as a fill-up gas. The results from these experiments performed at 525 K are shown in fig. 6. For $CO_2$ pressure dependence measurements the $H_2$ pressure was held at 34 kPa (256 Torr) and for the $H_2$ pressure dependence measurements the $CO_2$ pressure was held at 25 kPa (190 Torr). The measured data was fitted to eq. (1) to determine the coefficients $\alpha$ and $\beta$ for $H_2$ and $CO_2$ pressure dependencies. The solid lines in figs. 6A and 6B have been drawn using values of $\alpha = 0.9$ for $H_2$ pressures between 4 and 40 kPa and $\beta = -0.05$ for $CO_2$ pressure from 2.7 to 67 kPa. The dashed line between 40 and 76 kPa of $H_2$ pressure has been obtained with a value of $\alpha = -0.85$.

The surface composition of the cobalt foils was characterized by AES immediately after opening the reaction cell without any further heating of the sample. The carbon to cobalt and oxygen to cobalt AES peak height ratios after the reaction experiments are plotted in fig. 4 as a function of reaction temperature. The C/Co ratio drawn with open circles stays constant in the whole temperature range whereas the O/Co ratio starts to increase when temperature exceeds 540 K.

Table 1
Selectivity of $CO_2$ hydrogenation under various conditions on cobalt foil

| $T$ (K) | $H_2/CO_2$ ratio | $CH_4$ | $C_2H_6$ |
|---|---|---|---|
| 500 | 3 | 95 | 5 |
| 525 | 2 | 96 | 4 |
| 525 | 3 | 97 | 3 |
| 525 | 4 | 98 | 2 |
| 560 | 3 | 99 | 1 |

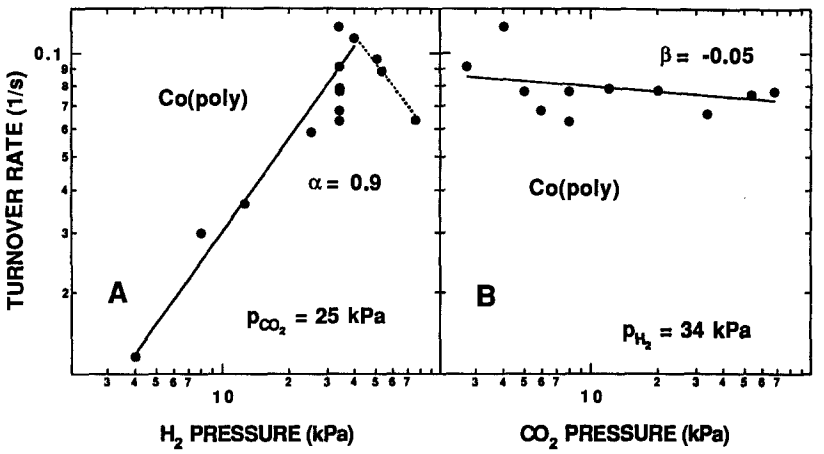


Fig. 6. Hydrogen (A) and carbon dioxide (B) partial pressure dependence on the rate of methane formation on cobalt foil. The reaction temperature was 525 K and the total pressure 101 kPa. The solid lines were drawn using eq. (1) with exponent values of $\alpha = 0.9$ and $\beta = -0.05$.

## 4. Discussion

### 4.1. SURFACE CARBON

Reactions of carbon layers with hydrogen have been studied on Fe [3,20], Ni [21–23] and Rh [7] surfaces. These carbon layers have been prepared using different methods like by running the CO + $H_2$ reaction several hours to obtain thick carbon layer on Fe [3,20], by exposing the surface either to $C_2H_2$ at 106 kPa and at 575 K (Rh) [7] or to CO at 3 kPa (Ni) [21]. Monolayer coverage of carbon on Ni has been achieved using only 20 L of CO [22] or by using segregation of carbon to the surface at 550 K in UHV [23]. Our method resembles the last idea though the carbon segregation in cobalt took place during the hydrogenation reaction in 101 kPa of $H_2$ at 450–560 K.

The rate of methane formation from carbon diffused onto the surface at 101 kPa $H_2$ and at 525 K was 0.022 methane molecules produced per cobalt site per second. On Fe foils Dwyer and Somorjai [3] report significantly higher rates at 575 K, and indicate that the rate of methane formation from carbon at the beginning equals the rate of CO hydrogenation. In our studies the rate difference between carbon and CO hydrogenation is about an order of magnitude. On Ni(100) the rate equals 0.008 methane molecules per second per site when calculated at 525 K [21]. On rhodium foil rates close to those on Ni have been observed exhibiting a value of 0.005 (site s)$^{-1}$ at 525 K [7]. The values observed on Ni and Rh surfaces are a factor of two smaller than what has been measured in CO hydrogenation. The difference in the rates of methane formation from C and CO in our measurements, can be explained, at least partially, by the limited segregation of C

onto the cobalt surface. The comparison of carbon hydrogenation data on Fe, Co, Ni, and Rh is displayed in table 2.

The activation energy of carbon hydrogenation on cobalt is $57 \pm 3$ kJ/mol between 450 and 530 K. This activation energy is smaller than what has been observed on Ni or Rh surfaces, about 88 kJ/mol [21,22,7], in the temperature range from 343 to 388 K for Ni and from 575 to 680 K for Rh.

At temperatures higher than 530 K the Arrhenius behavior of fig. 1 breaks off and also the carbon concentration observed in the post-reaction Auger spectra increases slightly. On Fe surfaces two regimes have been observed in the carbon hydrogenation, one, fast, corresponding to carbide hydrogenation and second, slow, corresponding to graphite hydrogenation [20]. Thus the decrease in the slope in fig. 1 can be explained by conversion of carbon segregating to the surface to graphite above 530 K resulting in slower hydrogenation rate. In CO hydrogenation the amount of carbon on the surface starts to increase when temperature exceeded 540 K with simultaneous onset of graphite formation.

The product distribution from the carbon hydrogenation showed 98 wt% methane and 2 wt% ethane above 500 K and only methane at temperatures lower

Table 2
Comparison of hydrogenation reactions on transition metals. The reaction temperature is 525 K and the total pressure 101 kPa if other values are not given. An asterisk (*) denotes extrapolated values

| Sample | Fe(foil) | Co(foil) | Rh(foil) | Ni(100), (111) |
|---|---|---|---|---|
| *$E_{act}$ (kJ/mol)* | | | | |
| C | – | $57 \pm 3$ | $88 \pm 13$ | $87 \pm 6$ |
| CO | $96 \pm 8$ | $86 \pm 10$ | $100 \pm 13$ | 103 |
| $CO_2$ | $71 \pm 8$ | $155 \pm 5$ | $67 \pm 8$ | 89 |
| *partial pressure dependence* | | | | |
| $H_2/CO$ | – | $1.5/-0.75$ | $1.0/-1.0$ [8] | – |
| $H_2/CO_2$ | – | $0.9/-0.05$ | 0.5/0.2 [8] | – |
| *selectivity to methane (wt%)* | | | | |
| C | $98.5^{560K}$ [20] | $98^{525K}$ | $100^{575K}$ | – |
| CO | $55^{560K}$ [4] | $80^{525K}$ | $84^{525K}$ | $93^{503K}$ |
| $CO_2$ at 575 K | 97 | 99 | 100 | – |
| *rate ($CH_4$ molecules/site s)* | | | | |
| C | $0.4^{600\ kPa}$ [3] | 0.02 | *0.005 | $*0.008^{13\ kPa}$ |
| CO | 0.4 | 0.33 !!! | 0.015 | $0.012^{16\ kPa}$ |
| $CO_2$ at 575 K | 10.9 | 1.55 | 0.36 | 0.06 |
| *main references* | | | | |
| C | | this work | [7] | [21,22] |
| CO | [3,4] | [12] | [7] | [6,28] |
| $CO_2$ | [3] | this work | [7] | [5] |

than 500 K. On Fe foil similar selectivity has been observed [20] but on Rh foil only methane is produced [7].

### 4.2. COMPARISON OF $CO_2$ HYDROGENATION ON COBALT, IRON, AND RHODIUM

The initial rates of methane formation in $CO_2$ hydrogenation at 525 and 575 K, when the $H_2/CO_2$ ratio was 3 and the total pressure 101 kPa (760 Torr), were 0.064 and 1.55 methane molecules produced per cobalt site per second, respectively. These results contradict the findings of Jnioui et al. [24] where turnover rates lower than 0.06 1/s for $CO_2$ hydrogenation on clean Co foil have been observed up to 770 K. After variable oxygen exposures prior to the $CO_2 + H_2$ reaction, they were able to observe turnover rates between 0.03 and 166 1/s at 525 K, the former corresponding to 3600 L of $O_2$ at room temperature and the latter to 101 kPa of $O_2$ at 770 K for 1 h. According to Jnioui et al. the reason behind the increased turnover rates is the subsurface oxygen that creates surface defects. We exclude the possibility of oxygen contamination on our cobalt foils by measuring the Auger-spectra before the reaction experiment. The O/Co peak height ratio before reaction experiments was $0.02 \pm 0.02$ corresponding to $1 \pm 1$ at% concentration [25] which is smaller than the O/Co peak height ratio of at least 0.05 reported for "clean" cobalt by Jnioui et al. [24]. The O/Co and C/Co peak height ratios after the reaction experiment were shown in fig. 4.

Turnover rates and activation energies for $CO_2$ hydrogenation on Co, Fe,Ni, and Rh can be compared using the collection of the data in table 2. Highest turnover rates for methane formation have been observed on Fe foils where the rate is almost seven times higher than that on cobalt at 575 K. The difference in the total pressure was six times higher in the Fe-experiment which can partly explain the difference. Rhodium catalysts show a factor of five lower turnover rates than cobalt under the same conditions and Ni surfaces are the slowest in this group of four.

The activation energy for methane formation in $CO_2$ hydrogenation on Co foil is $155 \pm 5$ kJ/mol and that for ethene formation $90 \pm 5$ kJ/mol. On cobalt catalysts precipitated from cobalt carbonate an activation energy of 88 kJ/mol for methane formation has been measured [26].

The activation energies in $CO_2$ hydrogenation can also be seen in table 2. The activation energy on cobalt, 155 kJ/mol, is significantly higher than that for Fe (71 kJ/mol) [3], Rh (67–71 kJ/mol) [7] or Ni (89 kJ/mol) [5] indicating a totally different rate limiting step for $CO_2$ hydrogenation on cobalt.

The selectivity towards methane, if CO is excluded, on cobalt at 570 K is about 99%. On iron at 570 K a value of 97% has been reported [3]. On rhodium foil the selectivity is 100% [7] which is slightly higher than on Co or Fe. In $CO_2$ hydrogenation almost only ethane has been seen as longer chain hydrocarbons.

The partial pressure dependence on small area catalysts has earlier been studied only on clean and $TiO_x$ covered Rh surfaces [8]. On clean Rh foil the value of the $H_2$ exponent was 0.5 which is lower than that on Co (0.9) and the $CO_2$ exponent was

0.2 which is higher than that of cobalt (−0.05). According to the analysis of the partial pressure data, the $CO_2$ hydrogenation on Rh was reported to proceed via CO and $H_2CO$ intermediates and the rate limiting step was the adding of the last hydrogen atom.

### 4.3. COMPARISON OF C, CO AND $CO_2$ HYDROGENATION

New insight in the reaction mechanism and rate limiting elementary reaction step in the hydrogenation reactions on cobalt can be gained by comparing the reactions of surface carbon, CO and $CO_2$. In fig. 7 is shown the comparison of the Arrhenius plots from these reactions. The activation energies are 57, 86 and 158 kJ/mol, for C, CO and $CO_2$ hydrogenation, respectively, indicating that the removing of oxygen from the C–O bond consumes energy.

The reaction mechanism for methane formation from CO and hydrogen on cobalt is reported to proceed via dissociation of CO on the surface [10,12,13]. Several reaction mechanisms for the $CO_2$ hydrogenation have been reported including direct hydrogenation of $CO_2$ [14], dissociation to CO and O [14], or to C and 2O [5,15] prior to the methane formation. In fig. 8 are shown the proposed reaction mechanisms for C, CO, and $CO_2$ hydrogenation based on our results. The common part in all the reaction mechanisms is the stepwise hydrogenation of carbon to methane. In the CO and $CO_2$ hydrogenation the common element is the formation of cobalt oxide on the surface and its reduction by hydrogen to form water. Based on the increase in the activation energy as the oxygen content of the reactants increases and the heats of formation shown in fig. 9, we propose that the rate limit-

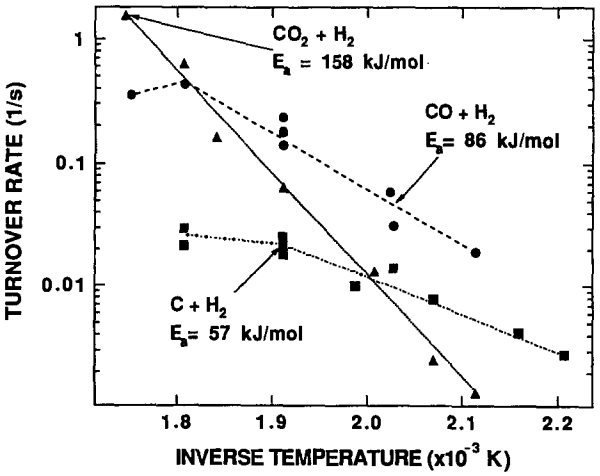


Fig. 7. Turnover rates on cobalt during hydrogenation of surface carbon (■), carbon monoxide (▲) and carbon dioxide (●). The hydrogen pressure was 101 kPa for C, 56 kPa for CO, and 76 kPa for $CO_2$ hydrogenation, the CO pressure 45 kPa and $CO_2$ pressure 25 kPa.

| C HYDROGENATION | CO HYDROGENATION | $CO_2$ HYDROGENATION |
|---|---|---|
| | $CO + * \leftrightarrow CO^*$ | $CO_2 + * \leftrightarrow CO_2^*$ |
| $H_2 + 2^* \leftrightarrow 2H^*$ | $H_2 + 2^* \leftrightarrow 2H^*$ | $H_2 + 2^* \leftrightarrow 2H^*$ |
| | | $CO_2^* + Co \leftrightarrow CO^* + CoO$ |
| | $CO^* + Co \leftrightarrow C^* + CoO$ | $CO^* + Co \leftrightarrow C^* + CoO$ |
| $C^* + H^* \leftrightarrow CH^* + *$ | $C^* + H^* \leftrightarrow CH^* + *$ | $C^* + H^* \leftrightarrow CH^* + *$ |
| $CH^* + H^* \leftrightarrow CH_2^* + *$ | $CH^* + H^* \leftrightarrow CH_2^* + *$ | $CH^* + H^* \leftrightarrow CH_2^* + *$ |
| $CH_2^* + H^* \leftrightarrow CH_3^* + *$ | $CH_2^* + H^* \leftrightarrow CH_3^* + *$ | $CH_2^* + H^* \leftrightarrow CH_3^* + *$ |
| $CH_3^* + H^* \leftrightarrow CH_4 + 2^*$ | $CH_3^* + H^* \leftrightarrow CH_4 + 2^*$ | $CH_3^* + H^* \leftrightarrow CH_4 + 2^*$ |
| | $CoO + H^* \rightarrow OH^* + Co$ | $CoO + H^* \rightarrow OH^* + Co$ |
| | $OH^* + H^* \leftrightarrow H_2O + 2^*$ | $OH^* + H^* \leftrightarrow H_2O + 2^*$ |
| | | or |
| | | $CO^* + H^* \leftrightarrow COH^* + *$ |
| | | $COH^* + H^* \leftrightarrow H_2CO^* + *$ |
| | | $H_2CO^* + Co \leftrightarrow CH_2^* + CoO$ |

Fig. 8. The reaction mechanisms proposed for C, CO and $CO_2$ hydrogenation. In the case of $CO_2$ hydrogenation two alternative reaction paths are given. The rate limiting step is shown with a one-way arrow ($\rightarrow$).

ing step in CO and $CO_2$ hydrogenation is the reduction of CoO that is formed during the cleavage of the C–O bond.

The energy changes shown in fig. 9 can be understood in the following way: The dissociation of C–O bond requires energy that is compensated by the formation of CoO of the surface. Methane formation from C and H releases 75 kJ/mol. The reduction of CoO by hydrogen to form water and Co releases only 2.5 kJ/mol and has a considerable energy barrier (240 kJ/mol per CoO) supporting strongly the idea of the reduction of CoO as the rate limiting step on these hydrogenation reactions.

In the case of $CO_2$ hydrogenation an alternate reaction path from CO to $CH_2$ is also given in fig. 8 that does not involve direct CO dissociation to show that the reduction of CoO can be the rate limiting step also within other reaction models.

Recently Iglesia et al. [16] have reported that addition of small amounts of Ru in the $Co/TiO_2$ catalysts increases the catalyst activity with no changes in the activation energy or reaction kinetics. Their explanations that Ru increases the reducibility of cobalt and enhances the removal of surface oxygen during the CO hydrogenation support the idea of CoO being the rate limiter on cobalt catalysts.

The formation on CoO and its slow reduction can also be the reason behind the low hydrogenation rates on Co/W(110) and Co/W(100) surfaces. Because these surfaces exhibit strained structures giving rise to high rate of CO dissociation, large amounts of C and O have been detected on the surface after the reaction in accordance with CoO formation [27].

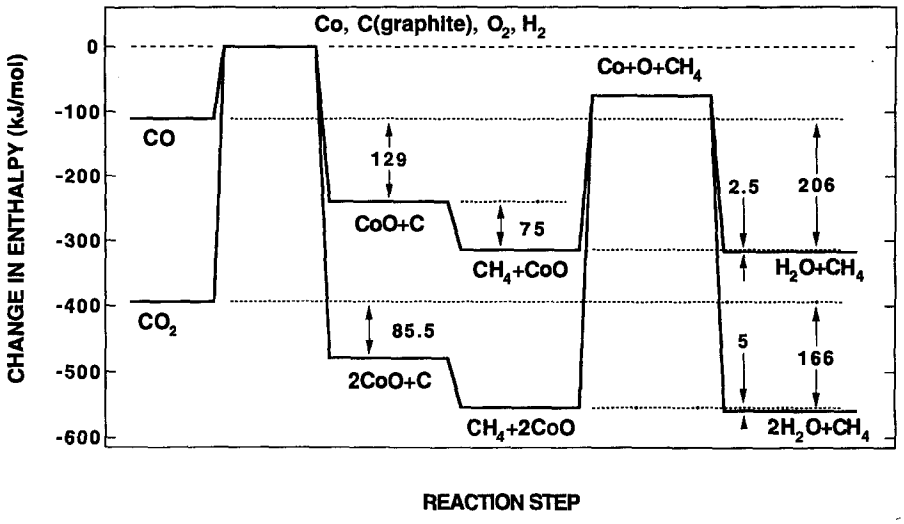


Fig. 9. The energy diagram of CO and $CO_2$ hydrogenation on cobalt calculated using the heats of formation. The dissociation of C–O bond requires energy that is compensated by the formation of CoO of the surface, releasing 129 and 85.5 kJ/mol for CO and $CO_2$, respectively. Methane formation from C and H releases 75 kJ/mol and the reduction of CoO 2.5 kJ/mol. The reduction of CoO has a considerable energy barrier and it is proposed to be the rate limiting step in the CO and $CO_2$ hydrogenation

Our previous data on Co/Au surfaces indicate positive partial pressure dependence of the rate of methane formation on both $H_2$ and CO [12]. The change in the sign of the reaction order in CO can be due to change in surface composition that enables quick CO dissociation on Co-sites and easy reduction of CoO due to the noble metal neighbors of the Co atom.

The product distributions at 525 K show that from C and $CO_2$ we get 98 and 97% methane and from CO only 80%. From C and $CO_2$ we obtain alkanes but from CO mainly alkenes as $C_2$–$C_4$ hydrocarbons. The product distributions for these three reactions on cobalt foils were shown in fig. 2. This trend of high rate of methane formation from C and $CO_2$ and longer chain hydrocarbon formation from CO is similar on all transition metals as can be seen from table 2, and thus the initiation of chain growth seems to be independent of the rate limiting step in the methane formation.

It should be noted that cobalt produces high molecular weight hydrocarbons at high conversions and under conditions used in the technology (higher reactant pressures and in the presence of promoters). Our experimental conditions are clearly inadequate to produce chain growth as a result of secondary polymerization reactions. We shall explore how high molecular weight products form from C, CO, $CO_2$ and hydrogen in future studies.

## 5. Conclusions

The following conclusions can be drawn from the results and evaluation of the present investigation:

(1) Activation energies for methane formation from surface carbon, carbon monoxide, and carbon dioxide on cobalt foils are $57 \pm 3$ kJ/mol, $86 \pm 10$ kJ/mol, and $155 \pm 5$ kJ/mol, respectively.

(2) The rate of methane formation on cobalt foil shows zero order partial pressure dependence on $CO_2$ and first order partial pressure dependence on $H_2$.

(3) Carbon and $CO_2$ hydrogenation produce mainly methane (>95%) with small amounts of ethane.

(4) The reaction proceeds via dissociation of C–O bonds and formation of CoO on the surface. The reduction of CoO is the rate limiting step in the CO and $CO_2$ hydrogenation reactions.

## Acknowledgement

This work was supported by the Director, Office of Energy Research, Office of Basic Energy Sciences, Material Science Division, US Department of Energy. One of us (JL) acknowledges the financial support of Neste Foundation.

## References

[1] R.B. Anderson, *The Fischer–Tropsch Synthesis* (Academic Press, New York, 1984).
[2] C.H. Bartholomew, Catal. Lett. 7 (1990) 303.
[3] D.J. Dwyer and G.A. Somorjai, J. Catal. 52 (1978) 291.
[4] H.J. Krebs, H.P. Bonzel and G. Gafner, Surf. Sci. 88 (1979) 269.
[5] D.E. Peebles, D.W. Goodman and J.M. White, J. Phys. Chem. 87 (1983) 4378.
[6] D.W. Goodman, R.D. Kelley, T.E. Madey and J.T. Yates Jr., J. Catal. 63 (1980) 226.
[7] B.A. Sexton and G.A. Somorjai, J. Catal. 46 (1977) 167.
[8] K.J. Williams, A.B. Boffa, M. Salmeron, A.T. Bell and G.A. Somorjai, Catal. Lett. 9 (1991) 415.
[9] J.A. Rodriguez and D.W. Goodman, Surf. Sci. Rep. 14 (1991) 1.
[10] J.J.C. Geerlings, M.C. Zonnevylle and C.P.M. de Groot, Surf. Sci. 241 (1991) 302.
[11] J.J.C. Geerlings, M.C. Zonnevylle and C.P.M. de Groot, Surf. Sci. 241 (1991) 315.
[12] J. Lahtinen, T. Anraku and G.A. Somorjai, J. Catal. 142 (1993) 206.
[13] P.K. Agrawal, J.R. Katzer and W.H. Manoque, Ind. Eng. Chem. 21 (1982) 385.
[14] G.A. Mills and F.W. Steffgren, Catal. Rev. 8 (1973) 159.
[15] S.-I. Fujita, H. Terunuma, M. Nakamura and N. Takezawa, Ind. Eng. Chem. Res. 30 (1991) 1146.
[16] E. Iglesia, S.L. Soled, R.A. Fiato and G.H. Via, J. Catal. 143 (1993) 345.
[17] E.L. Garfunkel, J. Parmeter, B.M. Naasz and G.A. Somorjai, Langmuir 2 (1986) 105.
[18] J. Lahtinen and G.A. Somorjai, J. Mol. Catal., submitted.
[19] J.-P. Hovi, J. Lahtinen, J. Vaari and R.M. Nieminen, Surf. Sci., submitted.

[20] H.J. Krebs and H.P. Bonzel, Surf. Sci. 99 (1980) 570.
[21] W.D. Goodman, R.D. Kelley, T.E. Madey and J.M. White, J. Catal. 64 (1980) 479.
[22] P. Finetti, R.G. Agostino, A. Derossi, A. Santoni and R. Rosei, Surf. Sci. 262 (1992) 1.
[23] H. He, J. Nakamura and K. Tanaka, Catal. Lett. 16 (1992) 407.
[24] A. Jnioui, M. Eddouasse, A. Amariglio, J.J. Ehrhardt, M. Alnot, J. Lambert and H. Amariglio, J. Catal. 106 (1987) 144.
[25] *Handbook of Auger Electron Spectroscopy*, 2nd Ed. (Physical Electronics Industries, Inc., 1976).
[26] H. Baussart, R. Delobel, M. Le Bras and J.-M. Leroy, J. Chem. Soc. Faraday Trans. 83 (1987) 1711.
[27] B.G. Johnson, C.H. Bartholomew and D.W. Goodman, J. Catal. 128 (1991) 231.
[28] R.D. Kelley and D.W. Goodman, Surf. Sci. 123 (1982) L743.